Final Master's project

Faculty of Veterinary Medecine (Universitat Autònoma de Barcelona)

Evaluation of the HETs formation in the progression of tuberculosis in the model of *Drosophila*

Bellaterra, 8 de septiembre del 2020

Presented by: Mireia Larrosa i Godall

Directed by: Dr. Pere Joan Cardona and Dr. Alberto Allepuz

El Dr. **PERE JOAN CARDONA,** principal investigador de la Unidad Experimental de Tuberculosis en el Institut de Recerca Germans Trias i Pujol (IGTP), i el Dr. **ALBERTO ALLEPUZ**, profesor agregado laboral de la Facultad de Veterinaria de la Universidad Autónoma de Barcelona (UAB),

Certifican que:

La memoria titulada "*Evaluation of the HETs formation in the progression of tuberculosis in the model of Drosophila melanogaster"* presentada por la estudiante **MIREIA LARROSA i GODALL** para la obtención del título de Máster en Zoonosis y una sola salud impartido por la Universidad Autónoma de Barcelona, se ha realizado bajo su supervisión y dirección. Considerándola acabada, autorizan su presentación para poder ser evaluada por la comisión correspondiente.

Mireia Larrosa i Godall
Firmado digitalmente por Mireia Larrosa i Godall
Fecha: 2020.09.08 18:57:04 +02'00'

Pere-Joan Cardona Iglesias
Firmado digitalmente por Pere-Joan Cardona Iglesias
Fecha: 2020.09.08 18:15:52 +02'00'

ALBERTO OSCAR ALLEPUZ PALAU
Firmado digitalmente por ALBERTO OSCAR ALLEPUZ PALAU
Fecha: 2020.09.08 18:35:09 +02'00'

Mireia Larrosa | Dr. Pere Joan Cardona | Dr. Alberto Allepuz

Summary

Abstract

Progression towards active tuberculosis (TB) has been linked to the formation of Neutrophilic Extracellular Traps (NETs) in mammals. This study evaluated the role of this mechanism in the TB model of *Drosophila Melanogaster* (Drosophila) after *Mycobacterium marinum* (*M.* marinum) inoculation in third instar larvae. After bacterial injection, *in vivo* and *in vitro* tracking of inflammatory cell dynamics associated with the infection was performed. To monitor the dynamics, the binary UAS-GAL4 system was used to create specific gain-of-function phenotypes. Notably, the filopodial formation was seen in both *in vitro* and *in vivo* samples, indicating morphological similarities with NETs formation. *In vitro*, filopodial extensions were associated with *M. marinum* bacteria, which suggests functional similarities with NETs. However, no DNA stained with DAPI was detected outside of the nuclei neither in viable cells nor disrupted cells, demonstrating that *Drosophila* larvae may not produce Hemocyte Extracellular Traps (HETs) after bacterial infection.

1. Introduction

Tuberculosis (TB) is a primary chronic lung infection mainly caused by *Mycobacterium tuberculosis* (*M. tuberculosis*). Although progress has been made regarding the prevention and control of TB infection, it is believed that *M. tuberculosis* has already infected a quarter of the world's population with an estimated 10 million cases and 1,5 million deaths annually (*Global Tuberculosis Report*, 2019). Although the greatest burden of the disease occurs in developing countries, developed countries are not spared from it (Ankrah *et al.*, 2018). Particularly, more than two-thirds of the global cases are reported in Africa and Asia. The main challenges for TB control rely on the HIV pandemic and the emergence of multi-drug resistant TB (Raviglione, *et al.*, 2016).

M. tuberculosis is a complex acid-fast bacillus slow-growing transmitted by aerosol inhalation from an infected individual. The bacillus can survive in a harsh microenvironment in the patient in a quiescent state, resulting in a latent TB infection (LTBI) (Ankrah *et al.*, 2018; Asay *et al.*, 2020). These bacilli remain dormant and reside within old lesions in the upper lobes of the lung. Reactivation of these dormant bacilli leads to active TB, which only occurs in 5-10% of patients (Ankrah et al., 2016; P. J. Cardona, 2009). The outcome depends on the immune status of the host, and results in a range of TB status from no infection, latent with subclinical disease, to active disease (Ankrah *et al.*, 2018). Furthermore, positron emission tomography (PET/CT) imaging revealed heterogeneity in lung pathology in LTBI patients, complicating the classification of *M. tuberculosis* infection into latent or active disease states. Due to this fact, biomarkers that predict disease progression are needed (Schnappinger, *et al.*, 2016). The population at risk of developing active TB (ATB) are those who are in continuously contact with a patient with ATB, or rather 6 hours (h) per day during the length of the diagnosis delay. This suggests that to acquire a ATB, is required a continuous reinfection process (Cardona, 2018).

1.1. Pathology and immune response to TB in humans

Pulmonary disease is present in more than 80% of TB cases. However, any part of the body can be affected. *M. tuberculosis* spreads through lymphatic, hematogenous, or direct extension from the infective focus. Although extrapulmonary TB (EPTB) occurs approximately in 20% of the cases, it can be seen in more than 50% of immunosuppressed populations (Ankrah *et al.*, 2018). Specifically, the pulmonary pathology includes, but is not limited to, inflammatory lesions, interstitial pneumonia, necrotic caseating granulomas encapsulated, non-cavitary necrotic

lesions, non-necrotic cellular lesions, and cavitary lesions. The heterogeneity of the lesions depends on the microenvironment where *M. tuberculosis* is located (Asay *et al.*, 2020).

1.1.1 Acquisition of *M. tuberculosis* infection

The infection is initiated when inhaled bacilli are phagocytosed by alveolar macrophages (AM), which are required to phagocytose toxic and inflammatory particles to minimize potential damage to the lung tissue (Russell, *et al.*, 2009). Several important barriers must be crossed for *M. tuberculosis* to reach the alveoli, most of which are poorly understood and often neglected (Scriba, *et al.*, 2017). Once inside the phagocyte, *M. tuberculosis* starts to grow and modulates the behavior of its phagosome by preventing its fusion with acidic, hydrolytically-active lysosomes through the secretion of early secretory antigenic target-6 (ESAT-6) and culture filtrate protein-10 (CFP-10) (Mitchell, *et al.*, 2016; Russell *et al.*, 2009). In other words, these peptides are the key to avoid the phagosome-lysosome union, and consequently, the apoptosis of the bacteria, allowing them to benefit from the internal milieu of the macrophages for growing until they cause necrosis (Cardona, 2017). Then, the initial phase of infection takes place. This phase is silent and occurs approximately 15 days before an initial pre-granuloma formation at the infection site (Cardona, 2015). The bacilli grow slow, duplicating every 24h until finally causing the necrosis, the apoptosis of the cell after around 6 days and the liberation of *M. tuberculosis* to the extracellular milieu. Extracellular bacilli are phagocyted by the neighboring AM, and the process is repeated until at least a bacterial load of 1000 bacilli is obtained, causing sufficient chemokine secretion to generate an inflammatory response. Inflammation allows the entrance of polymorphonuclear cells (PMN), neutrophils and monocytes, and the drainage of the infected AM to the lymph nodes. Once in the lymph nodes, *M. tuberculosis* is able to infect the macrophages, causing lymphadenitis, and the dendritic cells (Cardona, 2018).

The humoral response has been found to be very weak against LTBI. The weakness of this response against LTBI leads the host to induce a cellular immunity, giving the bacteria a better chance to grow until they cause necrosis of the macrophages and reinfect the host. Thus, an increased inflammatory response is induced, and macrophages (new growing sites for the bacilli) and neutrophils (source of cell membranes that induce FM) are attracted to the lesion site (Cardona, 2009). Specifically, sustained TNF signaling is required to maintain chemokine concentrations for cellular recruitment and retention (Russell *et al.*, 2009). This inflammatory cascade is regulated by a cellular response linked to the production of IFN-ϒ, which activates the infected macrophages causing the destruction of most of the replicating population of bacilli

(Russell, 2007). This cellular debris will be mixed with extracellular bacilli and become the first source of the non-replicating population of *M. tuberculosis* (Cardona, 2009).

Mature-phase granulomas show marked neovascularization and develop an extensive fibrotic capsule that delineates the margins between the macrophages, granulocytes, foamy macrophages, and giant cells, and the lymphocytic infiltrate (Ulrichs, *et al.*, 2006). In the late stages, the center of the granuloma loses its vascularization and becomes necrotic, which facilitates caseation.

1.1.2 Induction of the immune response in the lymph node

The accumulation of infected dendritic cells (DCs) in the regional lymph node promotes the development of the acquired immune response, through the presentation of epitopes (normally ESAT-6 and the antigen complex 85). This immune response is based mainly on the induction through the antigenic presentation of type 1 T helper (Th1) cells and a low proportion of $CD8^+$ T cells, able to recognize infected macrophages and activate them by secreting interferon ϒ (IFN- ϒ) (Russell *et al.*, 2009). Although, other $CD4^+$ T cell subtypes (Th2, Th17, or Treg) may be present depending on the chemokines and cytokines transported in the lymphatic drainage (Cardona, 2018). The delay of the T cell activation is suggested to be because the early stages of *M. tuberculosis* replication occur in compartments that do not promote antigen presentation to naïve $CD4^+$ T cells (Wolf *et al.*, 2008). Specific effector lymphocytes enter the systemic circulation and reach the infected lesions in the lung. Nevertheless, they will only be attracted to the lesion only if a big enough inflammatory response is generated. Thus, alveolar macrophages can be continually infected, even when specific effector lymphocytes are available, because they require a strong enough inflammatory response to attract them. Once the lymphocytes reach the infected lesion, the macrophages are activated, which kill the most intracellular bacteria. Nevertheless, a percentage of the bacilli enter in a non-replicating status and survive inside the necrotic tissue (Cardona, 2017).

1.1.3 *M. tuberculosis* extrapulmonary dissemination

The caused lymphadenitis after lymph nodes infection can progress and release bacilli to the efferent capillaries. Bacteria circulate through the circulatory system until the vena cava, where they can access the right atrium and ventricle, and finally, the lung where they can cause new sites of infection. Specifically, lung invasion occurs mainly through bacterial clumps and vascularization of previous lesions (Cardona, 2018). It is known that the vascularization formed in the *M. tuberculosis* lesions, are more permeable and fragile, allowing the bacteria to reinfect

and to spread towards the pulmonary capillaries (Osherov, *et al.*, 2016). Finally, *M. tuberculosis* can return to the circulation, arrive in the left atrium and ventricle, and spread throughout the body (Cardona, 2018).

To date, the mechanisms for extrapulmonary dissemination remain unknown (Qian *et al.*, 2018). However, it is noted that the bacilli's targets are related to vascularization characteristics. That is why the organs with higher vascularization and permeability, like bones in children or kidneys, are the most target organs (Cardona, 2018).

Another dissemination pathway is through the alveolar fluid drainage, which allows the bacteria to enter the pharyngeal cavity, and penetrate the mucosa in case of pre-existent lesions. This is the pathway that targets cervical ganglia or causes an intestinal ATB (Cardona, 2018).

1.1.4 The dynamic hypothesis of LTBI

M. tuberculosis infection causes a host immune response to isolate the bacilli in a granuloma, the hallmark of TB pathology. The quality of the granuloma depends on the bacillary load and the site at which the infection occurs, leading to two types of lesions: (a) the proliferative granuloma or "tubercle" is a lesion triggered by a low bacillary load and is formed by epithelial cells and fibroblasts. It soon progresses to fibrosis and calcification; (b) the exudative lesion or local neutrophil condensation is triggered by a high bacillary load, is favored in the upper pulmonary lobe, and is associated with the ATB (Cardona, 2009; Cardona, 2015). Specifically, the high bacillary load increases the risk of necrosis, forming a large progressive lesion, and favoring liquefaction, sloughing, and cavitation.

The proliferative granuloma is formed of a core of infected alveolar macrophages surrounded by foamy macrophages (FM), monocytes, and multinucleated giant cells (MGCs) (Kim *et al.*, 2010; Russell, 2007). Bacilli located inside the FM filled with lipid bodies, which indicates that they are at the end of their cycle, were able to start growing again and begin a new lesion. Particularly, FM are able to maintain a stressful environment that keeps the bacteria in a non-replicating state. This state helps the bacilli to survive future stressful environments more effectively (Cardona, *et al.*, 2003). Furthermore, the large number of fat bodies inside the FM and their interaction with the bacilli-containing phagosomes allow the bacteria to accumulate lipids in the form of triglycerides (TAG) (Cardona, 2009). Once the growing bacilli are controlled and most of the bacteria are in a non-replicating state, FM containing bacilli are drained to the upper bronchial tree by the alveolar fluid towards the gastrointestinal tract, where they would be swallowed, digested in the stomach, and be destroyed. However, a small

proportion of bacteria that can infect the internal aerosols (Cardona, 2009). The function of these aerosols is to condition the inspired air and avoid damage to the alveolar space. It is also important to mention that, in the alveolar fluid, the destroyed FM liberate lipids to the extracellular milieu which contribute to an increase of aerosols. The generation of the infected aerosols increases the chances of endogenous reinfections. This observation led to the "dynamic hypothesis" concept (Cardona, 2009).

This cycle is interrupted with the encapsulation and calcification of the granuloma, due to the action of the interlobular septa, or when neutrophils are attracted to the lesion, causing a higher degree of infiltration and cavitation (Cardona, 2017). Specifically, fibroblasts in the septa can detect lesions smaller than 1mm in the parenchyma. Consequently, fibroblasts encapsulate the lesion within 1-2 weeks (Cardona, 2017).

1.1.5 Role of the neutrophils in the ATB, the Bubble model

Previous studies found that C3HeB/FeJ infected with *M. tuberculosis* developed massive intragranulomatous necrosis (Kramnik, *et al.*, 2016). Further analysis of the lesion showed rapid increasing lesions due to the bacterial peripheral growth associated to infected FM surrounded by neutrophils (Cardona, 2017; Marzo *et al.*, 2014). Specifically, *M. tuberculosis* promoted the formation of Neutrophil Extracellular Traps (NETs), which is a mechanism to fight extracellular pathogens. However, in the case of *M. tuberculosis*, NETs are not able to destroy the bacteria and act as an extracellular growing site. From these primary lesions, satellite lesions appeared, which in time merged creating a massive lesion (Cardona, 2018; Prats, *et al.*, 2016). It is believed that this is an escaping mechanism that avoids encapsulation, increasing the risk of ATB development (Cardona, 2018). The process takes places in approximately 10 days and is known as the "bubble model" (Cardona, 2017).

TB tropism for the upper lobes can be explained by neutrophilic infiltration (Cardona, 2017). Because of gravity, the pulmonary upper lobes have a higher alveolar pressure and a higher diameter than the rest of the lung parenchyma, thus the capillary density is reduced. Moreover, it has less mobility and consequently, less lymphatic drainage which results in a lower immunological surveillance. Due to this fact, the upper lobes allow an increased accumulation of bacilli after the destruction of infected macrophages which increases the multiplicity of infection (MOI) of the arriving macrophages and favors the induction of necrosis and the accumulation of neutrophils at the site of the lesion (Cardona, 2015).

It has also been found that lesions in the upper lobes exhibit lower calcification which may be associated to a lower ability of the interlobular septum to react against minimal lesions as a result of the stress to which it is subjected and therefore encapsulate the lesion (Cardona, 2015; Suki *et al.*, 2013).

1.2. Main animal models used for TB research

Animal models are needed for understanding the humoral and cellular immune responses against *M. tuberculosis.* Previous studies observed that guinea pig, rabbit, rat, nonhuman primate (NHP), cattle, and goat mimic the features of the infection in humans. Particularly, mice and guinea pigs are the most widely used (Gong, *et al.*, 2020).

1.2.1 Mice

Although mice have similar immune responses as humans after *M. tuberculosis* infection, they present a different disease pathology. Bacilli reside mainly intracellularly in the lungs of the popularly used mouse strains, BALB/c, and C57BL/6, which leads to an inflammatory but non-necrotic lesion (Hoff *et al.*, 2011). Mouse strains vary in susceptibility to *M. tuberculosis* infection. C57BL/6 are more resistant than BALB/c in terms of survival time post infection, and C3HeB/FeJ demonstrated necrotic granulomas after infection in a study, which are more similar to the human's clinical features (Irwin *et al.*, 2015; Singh, *et al.*, 2018).

Mice have been the most used animals for vaccine discovery, and the C57BL/6 strain has been the most commonly used so far. However, the proven lung pathology similarity after infection with *M. tuberculosis* between C3HeB/FeJ mice model and human it's increasing its use as an *in vivo* evaluation model for new vaccine candidates. Additionally, the difference in immunological responses of mouse models and humans has promoted the development of humanized mice for TB research (Singh, *et al.* 2018).

1.2.2 Guinea pigs

Guinea pigs are an interesting animal model for TB because of their high susceptibility to infection with *M. tuberculosis.* The similarity in TB features between guinea pigs and humans has led to further drug and vaccine evaluation after initial screening in mice. Specifically, like humans, guinea pigs develop primary lesions after initial exposure that differ in morphology with the secondary legions that appear after the hematogenous dissemination of the acquired immunity. Additionally, guinea pigs develop rapidly progressing granulomas that are morphologically similar to humans, and Langerhans giant cells that are formed from macrophages and epithelioid cells. However, guinea pigs animal models are less commonly

used because they are more expensive and difficult to maintain than mice animal models, and there is restricted availability of immunological reagents (Gong *et al.*, 2020; Singh, *et al.*, 2018; Lenaerts *et al.*, 2007).

1.2.3 Rabbit

Rabbits mimic most of the pathological features in humans. Infection with *M. tuberculosis* is characterized by the development of heterogenous lesions in the same animal, similar to those described in humans: solid granulomas or nodules exclusively cellular, granulomas containing a caseous necrotic center, and older fibrotic lesions showing neovascularization. They are less susceptible to infection compared to guinea pigs, and their susceptibility depends on the strain. Recent studies have also indicated that virulence of *M. tuberculosis* strains determines the lesion severity in rabbit models. Rabbits are a suited model to demonstrate drug penetration, distribution, and cellular accumulation into well-structured TB lung lesions. However, they are not a very popular model because of their increased size and their biocontainment requirements (Gong et al., 2020; Kjellsson *et al.*, 2012; Singh, *et al.*, 2018).

1.2.4 Nonhuman primates (NHPs)

NHPs develop a similar pathology and disease condition to humans, indicating that immune responses of NHP models are very similar to those from humans (Gong et al., 2020). Also, NHPs are also the preferred model for simian immunodeficiency virus, making a suitable animal model to study HIV/TB coinfection. While *Cynomolgus macaques* are good models for latent TB because they are relatively resistant to *M. tuberculosis, Rhesus macaques* are more susceptible (Singh, *et al.*, 2018). Both are the most commonly used NHP for TB studies, such as evaluation of treatment efficacy, and vaccine development (Williams, *et al.,* 2016). Moreover, studies using PET/CT allowed a better understanding of the progression of infection to disease (Singh, *et al.*, 2018).

1.2.5 Zebrafish

Zebrafish are natural hosts of *Mycobacterium marinum* (*M. marinum*). In addition, after *M. marinum* infection, they develop granulomas which can degenerate and become necrotic, and generate immune responses composed of the same primary components as humans *(*Gong *et al.*, 2020). In this model, however, acquired immunity takes several weeks to develop while in mammals occur much faster (Williams, *et al.*, 2016). Finally, *M. marinum* infection in zebrafish models highlights the disease stages, including latency and reactivation, as observed in human TB (Singh, *et al.*, 2018).

1.3 *Drosophila melanogaster* as a model for TB research

The use of *Drosophila melanogaster* (*Drosophila*) as an animal model has been increasing in the past several years because of the following reasons: (a) *Drosophila* displays evolutionary conservation of innate immune responses and NF-kB signaling cascades; (b) the immune response can be measured in multiple ways, i.e. clotting, phagocytosis, melanization, and antimicrobial peptide (AMP) gene expression; (c) *Drosophila* is amenable to highly efficient screenings, relatively low cost, and no requirements for ethical approval (Mulcahy, *et al.*, 2011); and (d) it is characterized by a high susceptibility to tuberculosis caused by *M. marinum* (Jin *et al.*, 2017). Although *Drosophila* models of human diseases cannot replicate the entire disease process that occurs in humans, they possess rapid and simple genetics which allow studies to be carried out that would not be possible in larger animals (Dionne & Schneider, 2008).

Drosophila is a good model to understand the physiological consequences and associated immune response after *M. marinum* infection, along with anti-microbial drug discovery. However, the drawback of this model is that it can only be used to study the innate immunity due to the lack of adaptative immunity. Therefore, experimental results still need to be confirmed in mammals (Gong *et al.*, 2020).

1.4 Immune response of *Drosophila*

Although some things work differently in flies versus humans (i.e. signaling and binding systems), *Drosophila* innate immune responses have significant functional similarities with the vertebrate immune system (Dionne & Schneider, 2008; Mulcahy *et al.*, 2011).

The fruit fly has a multilayered immune system consisting of at least seven defensive mechanisms which may be encountered by the invading bacteria. Naming them from the outside to inside the fly body, these are: (a) the epithelia, the first physical barrier to infection, which recognizes infections and wounds, produce local AMPs, and send signals to the rest of the body (Tzou *et al.*, 2000); (b) the regulation of the gut's microbiota and invading pathogens through the production of AMPs which are produced in the fat body (the analog of the liver) and reactive oxygen species (ROS) (Ryu *et al.*, 2008); (c) the clotting response that seals wounds, prevents bleeding, and can physically trap bacteria (Scherfer *et al.*, 2006); (d) the phenoloxidase (PO) response which causes melanization at the site of an immune reaction through the release of ROS that lead to the activation of a systemic wound response mediated by the circulating hemolymph protease Hayan (Nam, *et al.*, 2012; Sugumaran, 2002); (e) the phagocytic response which is performed by specialized hemocytes directly through encapsulation or phagocytosis

of the invading bacteria, or indirectly by releasing systemic signals (Dijkers & O'Farrell, 2008); (f) the systemic AMP response where high concentration of AMPS are released into the circulation (Meister, *et al.*, 1997); and (g) the RNAi response which is required to control viral infections (X. Wang et al., 2006). (Dionne & Schneider, 2008; Mulcahy *et al.*, 2011).

1.3.1 Larval hemocytes

The haemocyte is a multifaceted cell involved in pathogen recognition, phagocytosis, cell signaling, production of antimicrobials peptides and immune compounds (Vlisidou & Wood, 2015). Previous studies based on *in vivo* tracking of hemocyte development through the GAL4-UAs system (Goto, *et al.*, 2003; Kimbrell, *et al.*, 2002), revealed three types of hemocytes in *Drosophila:* plasmatocytes, crystal cells, and lamellocytes (Honti, *et al.*, 2014).

Plasmatocytes are the main hemocyte in the larval circulation and are responsible for the recognition and engulfment of small particles, microbes, including invading bacteria, and apoptotic tissue. This function relies on the cell surface receptors such as Eater (Chung, *et al.*, 2011), NimC1 (Zsámboki *et al.*, 2013), and Draper (Fujita, *et al.*, 2012) that allow them to fight microorganisms. Plasmatocytes are also important for their role in the systemic immune response. Particularly, when plasmatocytes recognize the invading pathogen, protein Psidin is secreted, and consequently, AMP in the fat body is activated (Brennan, *et al.*, 2007; Honti, *et al.*, 2014). *Spatzle* (*Spz*) also have a role in the systemic immune response. Specifically, is a proinflammatory cytokine/mediator which links hemocytes and other immune-active tissues other than the fat body (Shia *et al.*, 2009). Plasmatocytes are functionally similar to mammalian monocytes, macrophages, and neutrophils (Anderl *et al.*, 2016). It has been estimated that larvae infected with 3000 CFUs of nonpathogenic bacteria, can eliminate approximately 95% of the bacterial load in 30min (Shia *et al.*, 2009). This facilitates bacterial elimination through AMP in the later stages and minimizes the risk of antimicrobial resistance developed by the pathogen (Makarova et al., 2016; Vlisidou & Wood, 2015).

Crystal cells are platelet-like cells, required for the melanization and blood clotting, and represent less than 5% of the larval circulating hemocytes. Crystal cells morphologically differ from plasmatocytes because they contain crystal inclusions of prophenoloxidase (PPO). During the melanization cascade, crystal cells are ruptured, releasing large quantities of PPO and molecules responsible for the lamellocytes differentiation into the hemolymph. PPO is the inactivated form of PO enzyme, which has a key role in melanization. This process depends on the JNK pathway (Bidla, *et al.*, 2007; Honti *et al.*, 2014).

Lamellocytes are not present in naïve larva's circulation, but their differentiation can be induced after specific stimulations. They are responsible for encapsulating large invaders that are too large to be phagocytized, like parasitoid eggs after wasp infection (Irving *et al.*, 2005). It has been suggested that injury of the epidermis or damage of the basal laminal is sufficient to induce hemocyte differentiation into lamellocytes (Honti *et al.*, 2014).

Finally, all contribute to capsule formation. Plasmatocytes form the inner layer of the capsule establishing tight junctions between membrane surfaces and serving as an adhesion basis for lamellocytes. Lamellocytes are responsible for the encapsulation, and crystal cells contribute to the melanization of the capsule.

None of these cell types is able to rearrange the DNA and somatic hypermutations to generate a cell type with immunological memory (Vlisidou & Wood, 2015). However, a recent study revealed that hemocytes of *Drosophila* adults mediate a specific "primed" immune response upon infection against *Streptococcus pneumoniae* that protects them against a second challenge of this same pathogen. This protective effect persists for the life of the fly and is mediated by phagocytes and the Toll pathway (Pham, *et al.*, 2007).

1.3.2 Hemocyte compartments of the *Drosophila* larva

There are three described hemocyte compartments in the *Drosophila* larva: the circulation, the lymph gland, and the sessile hematopoietic tissue.

The circulating hemocytes

The hemocytes are circulating in the hemolymph in an open circulatory system. More than 90% of the circulating hemocytes in a naïve larva are plasmatocytes. Furthermore, the number of circulating cells increases during larvae development (Honti *et al.*, 2014).

The lymph gland

Lymph glands are located on each side of the dorsal vessel and are composed of paired primary and secondary lobes. The primary lobe is divided into the cortical zone, which contains differentiated plasmatocytes and crystal cells, the medular zone, which contains the non-differentiated precursor cells, and the posterior signaling center that supervises the maintenance and differentiation of precursor cells (Anderl *et al.*, 2016). Until the late larval stage, naïve larvae's secondary lobe also contains precursor hemocytes, but when they are immune challenged, the lobe starts to present differentiated markers. During larvae-pupae transition, all types of hemocytes differentiate without immune induction, the lobes disrupt, and the differentiated cells enter in circulation (Honti *et al.*, 2014).

The sessile hematopoietic tissue

The sessile hematopoietic tissue is formed of a functional set of hemocytes located in the subepidermal layer of the body cavity, forming a striped pattern along the length of the larva. It contains plasmatocytes, crystal cells, and precursor hemocytes. Recent studies suggest that the adherence of the sessile hemocytes to the body involves a dynamic interaction: cells may enter the sessile hematopoietic tissue or leave to circulation. Although no signaling center has been identified to date, hemocyte density suggests a proliferating hemocyte pool at the posterior end of the larva. Furthermore, it was also proposed that hemocytes dwell in hematopoietic pockets, which may serve as hemocyte differentiation sites. These findings suggest that while lymph glands remain separated from the circulation, the sessile hemocytes might be mobilized more easily, either by immune or development signaling (Honti *et al.*, 2014).

1.3.3 The clotting response

Coagulation is the formation of an insoluble matrix in the blood or hemolymph that stops bleeding (hemostasis), assists wound healing, and protects against infection. Although the closed circulatory system in vertebrates require tight control over coagulation, the open circulatory system of insects permit coagulation to be more focused on quickly seal wounds, limit fluid loss, restore hydrostatic skeletons of soft body animals, and entrap microbes at wound sites (Dushay, 2009).

In *Drosophila* hemolymph coagulation, hemocyte extend both filopodia and blebs, which are only formed in absence of anticoagulant Ringer, demonstrating the importance of Ca^{2+} in clotting. Filopodia from hemocytes in the clot extend only a short distance, showing that most of the fibers consist of extracellular strands. Bacteria has been also proved to be associated with the *Drosophila* soft clot, however, it remained viable. PO role in in bacterial killing was not proved since the same amounts of dead bacteria were observed in wild type and *lz* mutants (Bidla, *et al.*, 2005).

Biochemistry and molecular genetics of clotting

The rapidity of hemolymph coagulation makes biochemical study of clotting factors difficult. Coagulation requires humoral and cellular proteins, which are provided by the fat body and hemocytes respectively. Proteomics and pull-down experiments have identified lipophorin, hexamerins, fat body protein 1, fondue (*fon*) and PO as the major humoral clotting factors in *Drosophila*. Plasmatocytes and crystal cells contribute to clotting by producing hemolectin

(*hml*), complement factor and PO. Triggin, factor also derived from hemocytes and the fat body, is also required for clotting (Scherfer *et al.*, 2004; Vlisidou & Wood, 2015).

The first clotting factors tested by functional genomics were *fon* and *hml*. *Fon*, a strong transglutaminase substrate, was confirmed as a clotting factor when RNAi knockdown of *fon* transcription caused a reduction of aggregation, strand draw-out, and affected wound healing (Dushay, 2009; Karlsson et al., 2004). The same effect was observed in the RNAi knockdown of transglutaminase and Ecdysone-induced gene 71Ee (Eig71Ee), suggesting an involvement of transglutaminase and its substrates *fon* and Eig761Ee (Dushay, 2009; Lindgren *et al*., 2008). *Hml* is a von Willebrand factor domain-bearing protein expressed by larval hemocytes. Loss of *hml* also abolished bead aggregation and caused a bleeding defect in larvae, which confirmed its role in coagulation and caused an increase of susceptibility to *Escherichia Coli* infection. However, *hml* mutant larvae survived wounding as well as control larvae, suggesting that *Drosophila* has redundant hemostatic mechanisms and which depend on the infectious agent and the host's physiology and ecology (Dushay, 2009; Lesch et al., 2007).

The clot formation is divided in two phases; initially, the wound is covered by a soft clot that is formed by aggregation of clot proteins cross-linked by transglutaminase. Subsequently, the clot matures and hardens through a PO-dependent response (Bidla, *et al.*, 2005; Vlisidou & Wood, 2015). Particularly, clot formation is initiated when plasmatocytes are activated to degranulation through unknown signaling, but hydroxide peroxide released at the wound site is a likely candidate (Theopold, *et al.*, 2014). Granules containing clotting factors such as *hml* and Eig716Ee, and plasma factors such as *fon* interact and are acted on by transglutaminase and possibly other factors in the presence of Ca^{2+} to produce the initial soft clot. Additional hemocytes adhere to the clot (Lesch *et al.*, 2007). Consequently, crystal cells are activated and ruptured to release PO triggered by endogenous signals like a negatively charged inner plasma membrane phospholipids. The PO melanizes the clot to produce its mature and stronger form. The JNK pathway, small GTPases and TNF homolog Eiger are also required for induction and rupture of crystal cells at the larval clot (Bidla *et al.*, 2007; Dushay, 2009).

Both transglutaminase activity and *fon* have been found on microbial surfaces in a spot-like manner. Further characterization showed also hexamerin and PO, suggesting a subset of the previously isolated clot components. Therefore, this spot-like aggregates were named "microclots"(Theopold *et al.*, 2014; Z. Wang *et al.*, 2010). Microclots aid to target transglutaminase to microbial surfaces, which facilitates the incorporation of the pathogens into

the clot matrix and prevents their dissemination and therefore septicemia. It is unknown how microbial surfaces are recognized, but it is likely that transglutaminase uses bacterial surface proteins as substrates and mediates their covalent linkage to microclots and the clot matrix (Wang *et al.*, 2010).

Drosophila clots are different from neutrophil extracellular traps

Vertebrate neutrophils play a key role against pathogens via phagocytosis, degranulation and by releasing DNA-containing neutrophil extracellular traps (NETs). NETs were first described in a novel immune response mechanism named NETosis where decondensed chromatin of neutrophils is released to the extracellular environment to bind and kill extracellular microorganisms. A similar mechanism has been reported in a wide variety of vertebrate and invertebrate cells which is termed ETosis and its webs extracellular traps (ETs) (Nascimento *et al.*, 2018).

These vertebrate ETs are similar to the insect clot in appearance, raising the question whether nucleic acids are involved in coagulation. Unlike *Galleria* larval clot stained with SYTOX Green (Bidla *et al.*, 2005) and *Periplaneta Americana* ETs stained with 4',6-diamidino-2-phenylindole (DAPI) (Nascimento *et al.*, 2018), no DNA was visible in *Drosophila* larval clots outside of the cell nuclei (Bidla, *et al.*, 2005; Dushay, 2009). Thus, despite the similarity in appearance and functionality, insect hemolymph clot and mammalian neutrophil NETs are quite different (Bidla et al., 2005). This difference could be attributed to differences between the clots in these species or differences in procedure or staining sensitivities of the two dyes (Dushay, 2009).

1.4 M. marinum infection in Drosophila

M. marinum is a pathogenic mycobacterium species that is genetically close-related to *M. tuberculosis* and causes TB-like disease in frogs and fish (Jin et al., 2017). Specifically, there is an 85% similarity between *M. tuberculosis* and *M. marinum* genome (Singh, *et al.*, 2018). However, because its optimal growth temperature (T) is 30^{o} C, it's capacity to cause disease in humans is limited, mainly focusing in areas with similar T like the skin where causes peripheral granulomatous disease (Cardona, 2018; Dionne *et al.*, 2006).

A low dose of *M. marinum* (50% lethal dose (LD_{50}) of 5 CFU) causes a lethal infection in *D. melanogaster* within a short period of time (Oh, *et al.*, 2013). After *M. marinum* infection in adults, the bacteria initially grow within the hemocytes and eventually escapes through an unknown mechanism, only to be phagocyted again. After a period of several days, the infection

undergoes a transition and the bacteria grows both inside and outside the cell (Dionne, *et al.*, 2003; Dionne *et al.*, 2006). Particularly, the early stage of the infection is characterized by bacterial growth within hemocytes which suggests that the early stages of *M. marinum* infection in the fly resemble the early stages of tuberculosis in human (Dionne, *et al.*, 2003). Around 96 hours post infection (hpi), bacterial growth pattern changes to the late stage, and the bacterial growth expand into large patches. New foci continue to appear until late in the infection. It is suggested that in the late stage, the infection focus it is found in many parts of the animal, specially head, legs and wings. Further examination of *M. marinum* in the phagocyte, suggested that the bacteria are capable of blocking acidification in *Drosophila*, just as they are in vertebrate macrophages (Barker, *et al.*, 1997). Finally, no extracellular bacterial cells were observed (Dionne, *et al.*, 2003).

1.4.1 Mechanisms by which *M. marinum* kills *Drosophila*

Metabolic regulation is linked to immune responses and inflammatory signaling. Prolonged or excessive immune activation can cause metabolic disruption and wasting of fatty and lean tissues. This effect is particularly seen in Gram-negative sepsis and in persistent bacterial infections such as TB (Clark *et al.*, 2013). *M. marinum* causes a progressive loss of energy reserves in *Drosophila* which is accompanied by hyperglycemia. It is caused by a systematic reduction in Akt activation, either by a reduction of the circulating insulin-like peptides or by an increase of the degradation of activated Akt. These two possibilities are not mutually exclusive. This consequently causes an excessive Gsk-3 and FOXO activity and an inability to produce new metabolic stores, which leads to a progressive loss of energy stores. The loss of energy stores has pathological effects. It is suggested that the observed impaired in insulin signaling in *M. marinum*-infected *Drosophila* might be a common response in many infections in many hosts. Moreover, is likely a significant cause of disease morbidity (Dionne *et al.*, 2006). The function of the link between immune activation and loss of anabolic signaling activity is unclear, particularly because FOXO is able to activate AMP expression, independently of the Toll and immune deficiency (IMD) pathways, but is not required for resistance to infection (Becker *et al.*, 2010).

1.4.2 Cytokine effect on mycobacterial resistance in *Drosophila*

Phagocytes produce cytokines which are a critical component of the cellular response to infection. In *Drosophila*, there are three genes that encode for IL-like signals: *upd1, upd2* and *upd3* (Agaisse, *et al.*, 2003). After a bacterial infection, *upd3* is secreted by phagocytes activating the JAK/STAT pathway in the fat body, where induces the expression of TotA, a

stress-induced peptide. This pathway is needed for antiviral defense, hematopoiesis, and to maintain gut integrity in response to bacterial infection.

A previous study showed that hemocytes produce *upd3* upon *M. marinum* infection which activates STAT signaling. This *upd3*-STAT signaling alters the interaction between mycobacteria and phagocytes through the reduction of *Atg2* expression, an autophagy gene. This leads to a reduction of the host lifespan and an impairment of the resistance against *M. marinum.* Specifically, overexpression of *Atg2* reduces by 50% the number of intracellular mycobacteria per cell and eliminated infection-induced phagocyte death by altering lipid deposition in immune cells and without significantly changing autophagy. It is known that *M. marinum* survival and/or proliferation is dependent on lipid accumulation in *Drosophila* phagocytes (Peán *et al.*, 2017).

2. Objectives

The main objective of this work was to study the granuloma formation and induction of HETs as a key mechanism of TB progression. To achieve this general goal, the following objectives were established:

- To characterize the injected volume of *M. marinum* in third instar *Drosophila* larvae.
- To study the evolution of the granuloma progression, and HETs induction in *M. marinum* infected *Drosophila* larvae.

3. Materials and methods

3.1 Characterization of the injected volume

The delivered volume was controlled through the pressure pulse, duration of the pressure pulse, and diameter of the needle. Ideally, for a particular size of the needle and a constant pressure and time, all larvae were expected to receive the same volume of sample. However, breaking the tip of the needles resulted of different tip sizes, ranged from 24.69 to 43.26 µm of inner diameter, and different needle tip angles that ranged from 85.42 to 89.61 µm. Therefore, the delivered volume of sample was normalized according to the needle diameter.

The needle characterization system was based on the characterization of the delivery system used by Zabihihesari, *et al.*, (2020). Particularly, the sample solution was injected into a Petri dish containing oil. The diameter of the injected droplet, the inner diameter of the used needle, and the angle of the needle tip were measured using ImageJ. Three measurements of each

parameter were made, and their respective mean was considered. Finally, the injected volume was assumed to be a function of the pressure (P), duration of the pressure (t), needle inner diameter (d), injected liquid viscosity (μ_1), oil viscosity (μ_2), interfacial tension between injected solution and oil (σ_1), interfacial tension between air and injected liquid (σ_2), and the angle of the needle tip (α).

$$\textbf{Eqn. 1} \quad V = f(P, t, d, \mu_1, \mu_2, \sigma_1, \sigma_2, \alpha)$$

The Buckingham Π was used to correlate the different parameters. Consequently, equation (Eqn) 1 was written as:

$$\textbf{Eqn. 2} \quad \frac{V}{d^3} = f\left(\frac{Pd}{\sigma_1}, \frac{\mu_1 d}{t\sigma_1}, \frac{\sigma_2}{\sigma_1}, \frac{\mu_1}{\mu_2}, \alpha\right)$$

Because the air, water and oil properties were considered constant, the Π groups $\frac{\sigma_2}{\sigma_1}$, $\frac{\mu_1}{\mu_2}$, α were assumed to remain constant in the study. This fact, reduced the Π groups to:

$$\textbf{Eqn. 3} \quad \frac{V}{d^3} = f\left(\frac{Pd}{\sigma_1}, \frac{\mu_1 d}{t\sigma_1}\right)$$

Constants c_1, c_2, and c_3 needed to characterize the injected volume were obtained from the correlation between the experimental data points and their correlated dimensionless injected volume represented in Fig. 1.

$$\textbf{Eqn 4} \quad \frac{V}{d^3} = c_1\left(\frac{Pd}{\sigma_1}\right)^{c_2}\left(\frac{\mu_1 d}{t\sigma_1}\right)^{c_3}$$

The nonlinear least squares method was used to determine the constants c_1, c_2, and c_3 in Eqn 4 based on the experimental data points. As a result, the following constants were obtained.

$$\textbf{Eqn. 5} \quad \frac{V}{d^3} = 870.36\left(\frac{Pd}{\sigma_1}\right)^{0.96}\left(\frac{\mu_1 d}{t\sigma_1}\right)^{0.53}$$

The interfacial tension between oil and water and the viscosity of water were considered to be $\sigma_1 = 26.3\ \frac{mN}{m}$ and $\mu_1 = 1\ mPa\ s$, respectively. Based on the correlation and the inner diameter of the needles, the pressure, and the time required to deliver 50µl of the reagent were determined in this experiment.

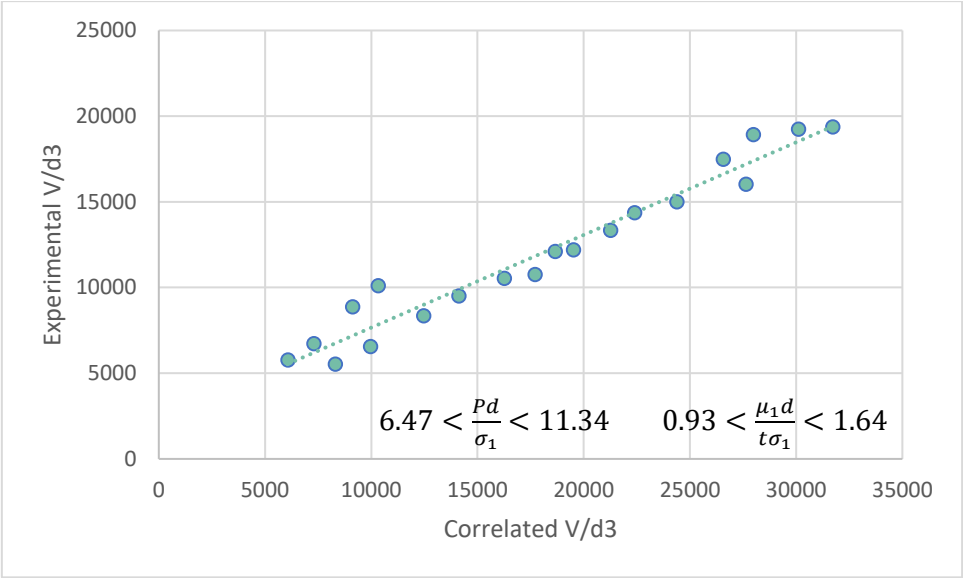

Fig 1. Comparison between the correlated dimensionless injected volume and the experimental results. P is the pressure, t is the duration of the pressure, d is the needle tip diameter, σ_1 is the interfacial tension between oil and injected liquid, and μ_1 is the viscosity of injected liquid.

3.2 Fly stocks and maintenance

All the experiments were carried out in stage three larvae of *Drosophila* Hml$^{\Delta}$-GAL4, UAS-GFP; He-GAL4 fed on standard yeast cornmeal food (Nutri-fly Bloomington formulation, Genesee scientific, USA). The fly stock was provided by Prof. Katja Brückner from the University of California San Francisco. The binary UAS-GAL4 system was used to create specific gain-of-function phonotypes in larval hemocytes. Second instar larvae were kept in an incubator at 29^{o}C during 4h for activation and were fed. After activation, larvae were transferred to a petri dish containing standard yeast cornmeal medium and were kept at 25^{o}C and 70% humidity with constant cycles of light and dark (12:12h).

3.3 Obtention of hemocytes from third instar *Drosophila* larvae

Hemocytes used in the present work were obtained from a total of 480 larvae, which were used in two different experiments (240n larvae/experiment): (i) *In vitro* infection where larvae were divided in three infection groups which were fixed at 4 different time points (3 hpi, 24 hpi, 48 hpi, and 72 hpi) and (ii) comparison between *in vivo* and *in vitro* infection, at each of the infection conditions, 60 larvae were fixed at 9 and 24 hpi. The experimental designs are summarized in Table 1 and 2 respectively.

	IN VITRO INFECTION		*IN VIVO* INFECTION	
EXTRACTION POINT	9hpi	24hpi	9hpi	24hpi
GROUP	Positive control (LPS)	Positive control (LPS)	Positive control (LPS)	Positive control (LPS)
	M. marinum	*M. marinum*	*M. marinum*	*M. marinum*
	Negative control (media)	Negative control (media)	Negative control (media)	Negative control (media)
NUMBER OF LARVAE	60	60	60	60

Table 1. Experimental design: *in vitro* visualization of ETs formation in infected third instar larvae

	IN VITRO INFECTION			
EXTRACTION POINT	9 hpi	24hpi	48hpi	72hpi
GROUP	Positive control (LPS)	Positive control (LPS)	Positive control (LPS)	Positive control (LPS)
	M. marinum	*M. marinum*	*M. marinum*	*M. marinum*
	Negative control (media)	Negative control (media)	Negative control (media)	Negative control (media)
NUMBER OF LARVAE	60	60	60	60

Table 2. Experimental design: comparison between *in vitro* and *in vivo* infection.

3.3.1 Hemolymph extraction

Third instar *Drosophila* larvae were placed into a 1.5mL microcentrifuge tube containing 500µL of sterile water, were rapidly vortexed, and were strained using a 40µm cell strainer (Falcon Scientific, United Kingdom). Ten of the previously activated larvae were transferred onto each well of a three-well slide and placed under the stereomicroscope with the dorsal-side facing up. 100µL of *Drosophila* Hemocyte Isolating Medium (DHIM) which contained 75% of Schneider's *Drosophila* medium and 25% of Fetal Bovine Serum (FBS) was added in each well of the slide. One set of forceps was placed on the posterior side of the larva to hold it in place and another one was used to disrupt the posterior cuticle open. Larvae were left to bleed in the well to allow the hemolymph to flow to the well. The pooled hemolymph was taken using a pipette and was ejected in a 0.5mL microcentrifuge tube kept in ice. The extraction process was repeated in the same well but with 50µL of DHIM. Finally, additional 50µL of DHIM was added to each well to wash the remaining hemocytes which was also ejected in the same microcentrifuge tube. It resulted in an hemocyte mixture of 200µL.

A 10µL of 1:1 Trypan Blue:hemocyte mixture was pipetted into the hemocytometer to count the number of live hemocytes. The concentration of hemocytes per milliliter was calculated using the following formula, where a, b, c and d are the number of live cells in each of the 4 counted corners of the hemocytometer.

$$\frac{Xcells}{mL} = \frac{a+b+c+d}{2} \cdot 10^4$$

12mm round cover glasses were placed in a 24 well-plate. The 200 µL of the hemocyte mixture were added at the desired concentration on each cover glass and the plate was incubated at 25ºC for 15min. Supernatant medium was removed from the well and it was washed with 200 of PBS 1x.

3.3.2 *Ex vivo* infection

LPS from *Escherichia Coli* (*E. Coli*) O111: B4 (500ng/well) was used as positive control and *M. marinum* (E11) presenting dsRed protein (10^6CFUs/well) as the experimental infection. Both conditions were diluted in DHIM containing Amphotericin B (Amph. B) and Kanamycin (Kan) antimicrobials in order to avoid contamination. DHIM containing only the supplemental antimicrobials was used as negative control. 200µL of each were added in its respective well of the 24well-plate for infection. After 1h of incubation, the media was removed from each well which were refilled with fresh DHIM containing Kan and Amph. B. The infected hemocytes were incubated at 25ºC for 3, 24, 48, and 72h.

3.3.3 *In vivo* infection

For larval injection, each third instar larva was placed on a small strip of filter paper moistened with 8µL of PBS located on a petri dish. The petri dish was coated with a 2.5% agarose gel to make the bottom rubbery and avoid breaking the glass needles through the injection of larvae. Larval dormancy was induced by placing the petri dish on ice for 1min before the injection. The *M. marinum* and LPS from *E. Coli* aliquots were thawed and diluted to obtain 500CFUs per injected volume in phosphate-buffered saline (PBS) and Brilliant Blue (BB). The injection was performed at an anterior position to the anal pads, preferably between the A6 and A7 segment, and using a 3.5” micro-capillary tube (Drummond Scientific Company, USA) connected to a Femtojet® 4i microinjector (Eppendorf, Germany). Following infection, larvae were incubated at 25º on fly medium (Nutri-fly Bloomington formulation, Genesee scientific, USA).

At 9hpi and 24hpi the larval hemolymph was extracted as explained before (3.3.1). However, in this case, the extraction was performed directly on a coverslip to avoid losing the *in vivo* formation of any ETs or clotting formation. The coverslip was placed on a petri dish and after the 15min incubation at 25ºC it was placed in a 24 well-plate after a PBS wash.

3.3.4 Sample fixation

Hemocytes were fixed with 4% of paraformaldehyde (PFA) during 20min at room temperature (RT) and were stained with DAPI. For imaging, coverslips were mounted on a glass slide with Fluoromount with the hemocytes facing down. The slide was left to dry overnight in the dark.

3.4 *In vivo* visualization of third instar *Drosophila* larvae

A total of 30 third instar larvae were infected as explained before (3.3.3) with 500CFUs of *M. marinum*, LPS as positive control and PBS as negative control. For imaging, at 24 hpi, larvae were carefully cleaned in water with a brush and mounted in a drop of ice-cold 100% glycerol on a three-well glass slide. Two glass slides contained a different infection group, resulting with 6 infected larvae per group. Silicone was used to fix the cover slip onto the larvae. The mounted larvae were kept at -20^{o}C for 45 minutes prior imaging to guarantee larval dormancy.

	EXTRACTION POINT	GROUP			NUMBER OF LARVAE
IN VIVO INFECTION	24 hpi	Positive control (LPS)	*M. marinum*	Negative control (media)	30

Table 3. Experimental design: *in vivo* visualization of ETs formation in infected third instar *Drosophila* larvae.

3.5 Microscopy and image analysis

Confocal microscopy measurements of live *Drosophila* larvae and pulled hemocytes were performed on the Abberior Instruments STEDYCON microscope (Abberior Instruments GmbH, Germany) mounted on Nikon Ti2-U inverted microscope body (Nikon Instruments Europe BV, Netherlands) using 488 and 561 nm excitation laser sources for EGFP and dsRed fluorescent proteins, respectively. The fluorescence excitation and signal collection were performed using a 100×/1.45 numerical aperture (NA) CFI Plan Apochromat Lambda oil immersion objective (Nikon Instruments Europe BV). Following acquisition, images and corresponding z-stacks were processed using Fiji (ImageJ distribution) software.

4. Results

4.1 Imaging of *in vitro* infected hemolymph

Imaging of larval hemocytes fixed at 3hpi showed high concentration of cells extending filopodia, both in the clot and outside the clot. Filopodia were longer on hemocytes outside the clot and were only extended in a single horizontal plane (z stack). However, morphological differences were found between infection groups (Fig. 2A, 2B and 2C): (i) clotting formation was seen in almost all the hemocytes infected with LPS and *M. marinum*. Nevertheless, filopodia extension was hardly seen in the negative sample; (ii) length of the extended filopodia

was larger in LPS-induced hemocytes followed by *M. marinum* infected cells. Non-infected hemocytes barely extended filopodia.

The association of bacteria with the clot prevents their dissemination and avoids infection of wounded larvae. As it is seen in Fig. 2C, bacteria were found associated with the clot. Particularly, hemocytes infected with *M. marinum* containing dsRed protein showed that most of the bacteria remained outside and surrounding the hemocyte rather than being phagocytized.

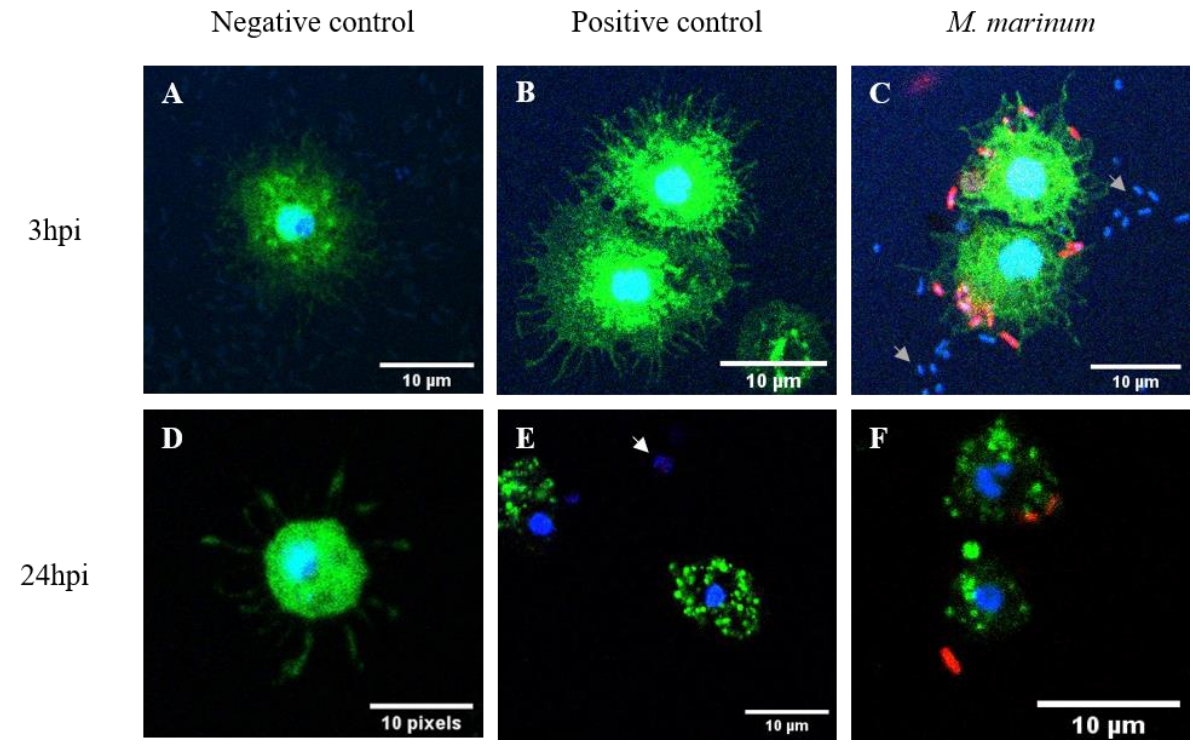

Fig 2. Induced clotting formation analysis of extracted hemolymph. Imaging was performed by confocal microscopy at 100x. Green represents hemocytes expressing GFP-hemolectin, blue is DAPI stained DNA and red is *M. marinum* expressing dsRed protein. Grey arrows point to yeast stained with DAPI which resulted from larval microbiota during the extraction. White arrow indicates dead cells which do not present green fluorescence. Tridimensional imaging of Fig. 2C is found in the annexes (Fig. A5).

Most of the hemocytes seen in all the samples fixed at 24hpi showed disrupted cellular morphology (Fig. 2D, 2E and 2F). Nevertheless, cells that barely extended filopodia remained viable. Thus, most of the viable cells were seen in the negative sample. Dead cells did not present green fluorescence. 48hpi presented similar appearance (data not shown) with reduced fluorescent stimulation suggesting no cellular viability after this time point. Wells containing larval hemocytes incubated until 72hpi presented unknown fungal contamination. Therefore, imaging analysis was not performed.

4.2 Imaging of in vivo infected hemolymph

Hemocytes extracted at 9 hours after *in vivo* infection presented similar morphology as *in vitro* infected hemolymph fixed at 3hpi. However, despite performing the extraction directly on the coverslip, shorter filopodia were formed. Furthermore, plasmatocytes from *M. marinum* and LPS inoculated larvae showed large intracellular vesicles of different size and shape but they were rarely seen in the negative control sample.

Hemolymph extracted from infected larvae at 24hpi showed disrupted hemocytes which were barely detected by the confocal microscope (Fig. A3). Moreover, ellipsoidal shaped structures with extended filaments were also seen in the sample (Fig. A4). No bacteria were observed in any of the *M. marinum* infected samples.

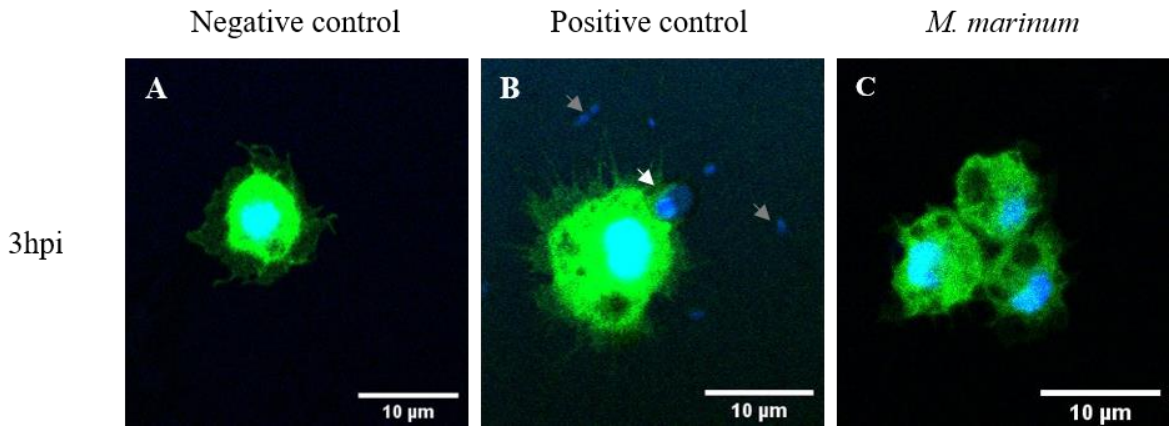

Fig 3. Clotting formation analysis of extracted hemolymph at 9 hours after *in vivo* infection of third instar *Drosophila* larvae. Imaging was performed by confocal microscopy at 100x. Green represents hemocytes expressing GFP-hemolectin and blue is DAPI stained DNA. Grey arrows point to yeast stained with DAPI which resulted from larval microbiota during the extraction. White arrow indicates dead cells which do not present green fluorescence.

4.3 Imaging of live Drosophila larvae inoculated with M. marinum

The main objective of performing live imaging of *Drosophila* larvae is to observe the changes in the hemocytes distribution, conformation, and morphology. Observation of the hole larvae at 24hpi showed higher amounts of circulating hemocyte both in *M. marinum* and LPS infected larvae in comparison with the negative control (Supplementary Fig. A1). Moreover, hemocyte distribution pattern was disturbed as a result of the infection. Normally in non-infected larvae hemocytes are localized in the subepidermal stripped pattern named sessile hematopoietic tissue and in the proliferative hemocyte pool localized found in the posterior part of the larvae, above the anal pads (distribution seen in Fig. A1a).

As it is seen in Fig. 3, hemocytes of larvae elicited with LPS and *M. marinum* (Fig. 3A and 3B, respectively) started to extend filopodia and blebs at 24hpi. Unlike clotting formation observed

after hemolymph extraction, filopodial extension in live larvae were presented in a tridimensional form.

Despite morphological changes in hemocytes such as intracellular vesicles were seen in all the infection groups, no clotting formation was detected in the negative control (Fig. 3C). It is important to highlight that *M. marinum* infected larvae presented higher amount and bigger intracellular vesicles. Lastly, no bacteria were found in any of the live infected larvae.

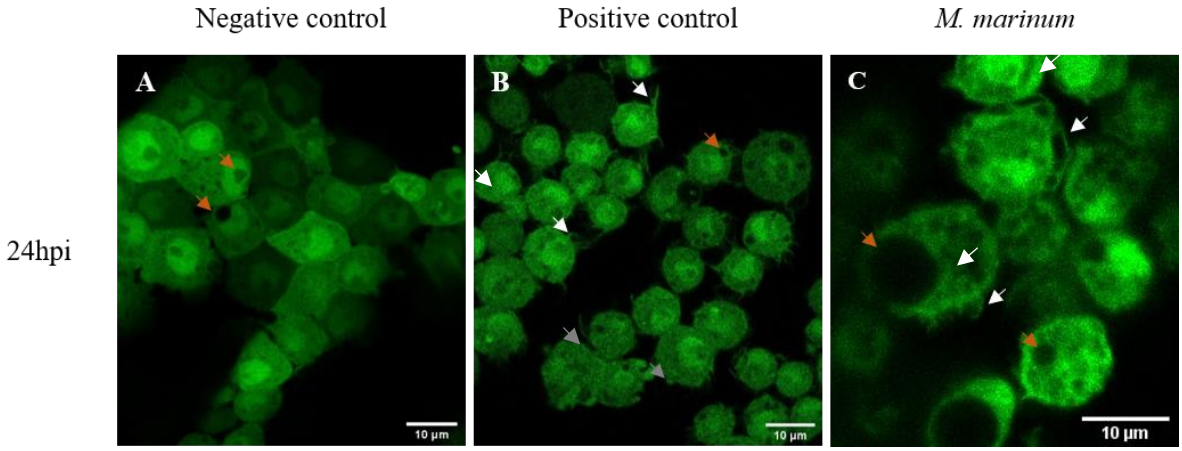

Fig 4. Imaging of live third instar *Drosophila* larvae at 24hpi performed with confocal microscopy. White arrows indicate the extended filopodia, grey arrows point to extended blebs, orange arrows indicate intracellular vesicles, and green represents GFP-hemolectin hemocytes. Distribution and morphology of hemocytes after inoculation with (A) PBS as negative control, (B) LPS as positive control, and (C) *M. marinum*.

4.4 Drosophila clots are different from NETs

A remarkable feature of the NETs formation is the presence of extracellular DNA and the ability to kill bacteria. Despite the morphological and functional similarities with the *Drosophila* clot, no DNA outside of the cell nuclei was detected in any of the analyzed samples stained with DAPI. Thus, despite the similarities, *Drosophila* hemolymph clot is different from mammal NETs.

5. Discussion

Drosophila is a well-established model to study the innate immune response. The innate immune response is the first line of defense against pathogen and environmental challenges (Sorvina *et al.*, 2013). Unfortunately, there is very little understanding of its dynamics, especially *in vivo*. Towards this aim, visualization of the response to bacterial infection of the circulating hemocytes response in intact and live *Drosophila* larvae was performed. However, to gain image specificity, ex vivo studies were also performed, which were carefully designed to reflect *in vivo* conditions.

Images obtained from live larvae allowed us to analyze the overall cell morphology and distribution of these cells inside the larval body. Unfortunately, the lack of bacterial signaling, mainly due to the low infectious dose, did not allow to monitor the presence and distribution of bacteria. The high sensitivity of the larvae against *M. marinum* infection forced the reduction of the infectious dose up to 500CFUs/larva to guarantee larval survival until 24hpi, which made almost impossible the detection of live bacteria. However, this could be overcome by the inoculation of a higher infectious dose and early stage monitoring of bacterial progression. A previous study described the formation of intracellular vesicles in hemocytes after infection in *in vivo* larvae, which appeared to be related to phagosomes instead of secretory vesicles (Sorvina *et al.*, 2013). At 24hpi, a significant increase in the size and number of intracellular vesicles after *M. marinum* and LPS infection was observed. Even though these results cannot be related to intracellular bacteria and phagocytosis, vesicle stimulation after infection compared with negative control larvae supports this theory.

Filopodia formation seen in the negative sample suggests that some of the conditions to which hemocytes were exposed did not fully reflect *in vivo* circumstances. Unlike ex vivo experiments performed by Bidla *et al.*, (2005), hemolymph was diluted, and therefore its components were present at a different concentration as in the live larvae. However, to avoid the rapid melanization observed during the methodological design, dilution of hemolymph in 200µL was needed. Differences observed in the direction of the extended filopodia in *in vivo* and *in vitro* imaging may also result from *ex vivo* conditions such as the plasmatocytes adhesion to the coverslip surface. While hemocytes adhere to the coverslip surface, hemolymph bled on a coverslip mostly clots and melanizes at its interface air (Butt & Shields, 1996) as it would happen at a wound site. Thus, the hanging drop method would expose the hemocytes to a higher oxygen concentration and surface tension (Bidla *et al*., 2005), allowing the filopodia to extend also in a vertical plane. Further studies using phase contrast microscopy are needed to better understanding of the role and morphology of both filopodia and strands after *M. marinum* infection.

Hemolymph extraction after *in vivo* larvae challenge aimed to reflect *in vivo* conditions as much as possible easing image obtention. It is important to state that larval dormancy achieved through keeping larvae at -20^{o}C was achieved in 60% of the cases. Depending on the larva size, stage, and infection conditions (among others), larval susceptibility to freezing temperatures varied making it harder to achieve immobilization without causing the larva to die. Nevertheless, clotting formed in this case showed less and shorter filopodial extensions. The

decreased cellular response may be explained by the difference in the challenged bacterial CFUs or due to the fibers' fragility. NETs have been described as very fragile fibers and hard to preserve during washings and fixing procedures (Brinkmann *et al.*, 2004). Therefore, similarities in morphology suggest that filopodia extensions fragility may cause reduced clotting formation. Extractions were performed directly to the coverslip to minimize hemolymph manipulation and, consequently, the destruction of fibers formation. However, it may not be enough.

NETs formation appears to be a form of innate response that is characterized by the presence of extracellular DNA and the capacity to kill bacteria (Brinkmann *et al.*, 2004). Obtained results confirmed that no DNA stained with DAPI was visible in the clot matrix outside the nuclei at an early stage after bleeding, as it was described by Bidla *et al.*, (2005). Moreover, it has also been reported that PO Thus, *Drosophila* hemolymph clot, and mammalian NETs are quite different. Data obtained since 24hpi of *in vitro* infected hemolymph strongly indicates that HETs are not a result of leakage during cellular disintegration and therefore *Drosophila* hemocytes may not produce HETs. However, HETs formation as a result of cellular death after more prolonged infections cannot be excluded. This would determine the role of *Drosophila* as an animal model for TB progression to ATB. In this study, it is important to highlight that HETs were only considered if they followed two requirements: the presence of extracellular DNA-containing fibers and the ability to kill bacteria. Characterization of the differences in both concepts is needed in insects as they are similar in functionality and morphology and differ among species and stages.

Further studies need to be done to confirm the absence of HETs formation in *Drosophila* larvae and characterize the dynamics of the clot formation in *in vivo* larvae in correlation with live bacteria.

6. Conclusions

Circulating hemocytes stimulation, intracellular vesicles and clot formation were demonstrated in *Drosophila* larval hemolymph after LPS and *M. marinum* infection. However, no extracellular DNA was seen at the clot matrix and after cell destruction which may indicate that *Drosophila* hemocytes may not produce HETs.

7. Acknowledgements

I would like to thank Institut Germans Trias I Pujol (IGTP) institution for giving me the change to perform this project, especially to the Experimental Tuberculosis Unit (UTE) where it has been achieved. Particularly, I would like to show my gratitude to Marta Arch and Esther Fuentes for being always and my disposal, for their patience and for letting me learn from their knowledge and their wisdom. I would like to thank Jakub Chojnacki as well (IrsiCaixa AIDS Research Institute, Barcelona) for the help with the fluorescent microscopy images acquisition. Also, to Dr. Pere Joan Cardona for sharing his experience with me and for giving me the confidence to achieve my professional goals. Lastly, express thanks to everyone who supported me and helped me during this study.

8. References

Agaisse, H., Petersen, U., Boutros, M., Mathey-prevot, B., & Perrimon, N. (2003). Signaling Role of Hemocytes in Drosophila JAK / STAT-Dependent Response to Septic Injury. *Cell Press*, *5*, 441–450. https://doi.org/https://doi.org/10.1016/S1534-5807(03)00244-2

Anderl, I., Vesala, L., Ihalainen, T. O., Vanha-aho, L. M., Andó, I., Rämet, M., & Hultmark, D. (2016). Transdifferentiation and Proliferation in Two Distinct Hemocyte Lineages in Drosophila melanogaster Larvae after Wasp Infection. *PLoS Pathogens*, *12*(7), 1–34. https://doi.org/10.1371/journal.ppat.1005746

Ankrah, A. O., Glaudemans, A. W. J. M., Maes, A., Van de Wiele, C., Dierckx, R. A. J. O., Vorster, M., & Sathekge, M. M. (2018). Tuberculosis. *Seminars in Nuclear Medicine*, *48*(2), 108–130. https://doi.org/10.1053/j.semnuclmed.2017.10.005

Ankrah, A. O., van der Werf, T. S., de Vries, E. F. J., Dierckx, R. A. J. O., Sathekge, M. M., & Glaudemans, A. W. J. M. (2016, April 1). PET/CT imaging of Mycobacterium tuberculosis infection. *Clinical and Translational Imaging*. Springer-Verlag Italia s.r.l. https://doi.org/10.1007/s40336-016-0164-0

Asay, B. C., Edwards, B. B., Andrews, J., Ramey, M. E., Richard, J. D., Podell, B. K., … Lenaerts, A. J. (2020). Digital Image Analysis of Heterogeneous Tuberculosis Pulmonary Pathology in Non-Clinical Animal Models using Deep Convolutional Neural Networks. *Scientific Reports*, *10*(1), 1–14. https://doi.org/10.1038/s41598-020-62960-6

Barker, L. P., George, K. M., Falkow, S., & Small, P. L. C. (1997). Differential Trafficking of Live and Dead Mycobacterium marinum Organisms in Macrophages Downloaded from. *INFECTION AND IMMUNITY*, *65*(4), 1497–1504. https://doi.org/10.1128/IAI.65.4.1497-

1504.1997

Becker, T., Loch, G., Beyer, M., Zinke, I., Aschenbrenner, A. C., Carrera, P., … Hoch, M. (2010). FOXO-dependent regulation of innate immune homeostasis. *Nature*, *463*, 369–373. https://doi.org/10.1038/nature08698

Bidla, G., Dushay, M. S., & Theopold, U. (2007). Crystal cell rupture after injury in Drosophila requires the JNK pathway, small GTPases and the TNF homolog Eiger Gawa. *Journal of Cell Science*, *120*, 1209–1215. https://doi.org/10.1242/jcs.03420

Bidla, G., Lindgren, M., Theopold, U., & Dushay, M. S. (2005). Hemolymph coagulation and phenoloxidase in Drosophila larvae. *Developmental and Comparative Immunology*, *29*(8), 669–679. https://doi.org/10.1016/j.dci.2004.11.007

Brennan, C. A., Delaney, J. R., Schneider, D. S., & Anderson, K. V. (2007). Report Psidin Is Required in Drosophila Blood Cells for Both Phagocytic Degradation and Immune Activation of the Fat Body. *Current Biology*, *17*, 67–72. https://doi.org/10.1016/j.cub.2006.11.026

Brinkmann, V., Reichard, U., Goosmann, C., Fauler, B., Uhlemann, Y., Weiss, D. S., … Zychlinsky, A. (2004). Neutrophil Extracellular Traps Kill Bacteria. *Science*, *303*(5663), 1533–1535. https://doi.org/https://doi.org/10.1126/science.1092385

Butt, T. M., & Shields, K. S. (1996). The structure and behavior of gypsy moth (Lymantria dispar) hemocytes. *Journal of Invertebrate Pathology*, *68*(1), 1–14. https://doi.org/10.1006/jipa.1996.0052

Cardona, P.-J. (2009). A dynamic reinfection hypothesis of latent tuberculosis infection. *Infection*, *37*(2), 80–86. https://doi.org/10.1007/s15010-008-8087-y

Cardona, P.-J. (2017). What We Have Learned and What We Have Missed in Tuberculosis Pathophysiology for a New Vaccine Design: Searching for the “Pink Swan.” *Frontiers in Immunology*, *8*(556), 1–11. https://doi.org/10.3389/fimmu.2017.00556

Cardona, P.-J. (2018). Patogénesis de la tuberculosis y otras micobacteriosis. *Enfermedades Infecciosas y Microbiología Clínica*, *36*(1), 38–46. https://doi.org/10.1016/j.eimc.2017.10.015

Cardona, P.-J., Gordillo, S., Díaz, J., Tapia, G., & Amat, I. (2003). Widespread Bronchogenic Dissemination Makes DBA / 2 Mice More Susceptible than C57BL / 6 Mice to Experimental Aerosol Infection with Mycobacterium tuberculosis. *Infection and Immunity*, *71*(10), 5845–5854. https://doi.org/10.1128/IAI.71.10.5845

Cardona, P. J. (2015). The key role of exudative lesions and their encapsulation: Lessons learned from the pathology of human pulmonary tuberculosis. *Frontiers in Microbiology*,

6(612), 1–8. https://doi.org/10.3389/fmicb.2015.00612

Chung, Y.-S. A., & Kocks, C. (2011). Recognition of Pathogenic Microbes by the Drosophila Phagocytic Pattern Recognition Receptor Eater * □ S. *The Journal of Biological Chemistry*, *286*(30), 26524–26532. https://doi.org/10.1074/jbc.M110.214007

Clark, R. I., Tan, S. W. S., Péan, C. B., Roostalu, U., Vivancos, V., Bronda, K., … Dionne, M. S. (2013). XMEF2 is an in vivo immune-metabolic switch. *Cell*, *155*, 435–447. https://doi.org/10.1016/j.cell.2013.09.007

Dijkers, P. F., & O'Farrell, P. H. (2008). Drosophila Calcineurin Promotes Induction of Innate Immune Responses. *Current Biology*, *17*(23), 2087–2093. https://doi.org/doi.org/10.1016/j.cub.2007.11.001

Dionne, M. S., Ghori, N., & Schneider, D. S. (2003). Drosophila melanogaster is a genetically tractable model host for Mycobacterium marinum. *Infection and Immunity*, *71*(6), 3540–3550. https://doi.org/10.1128/IAI.71.6.3540-3550.2003

Dionne, M. S., Pham, L. N., Shirasu-Hiza, M., & Schneider, D. S. (2006). Akt and foxo Dysregulation Contribute to Infection-Induced Wasting in Drosophila. *Current Biology*, *16*(20), 1977–1985. https://doi.org/10.1016/j.cub.2006.08.052

Dionne, M. S., & Schneider, D. S. (2008). Models of infectious diseases in the fruit fly Drosophila melanogaster. *Disease Models and Mechanisms*, *1*(1), 43–49. https://doi.org/10.1242/dmm.000307

Dushay, M. S. (2009). Insect hemolymph clotting. *Cellular and Molecular Life Sciences*, *66*, 2643–2650. https://doi.org/10.1007/s00018-009-0036-0

Fujita, Y., Nagaosa, K., Shiratsuchi, A., & Nakanishi, Y. (2012). Role of NPxY motif in Draper-mediated apoptotic cell clearance in Drosophila. *Drug Discoveries & Therapeutics*, *6*(6), 291–297. https://doi.org/10.5582/ddt.2012.v6.6.291

Global Tuberculosis Report 2019. (2019). Geneva. Retrieved from http://apps.who.int/bookorders.

Gong, W., Liang, Y., & Wu, X. (2020). Animal Models of Tuberculosis Vaccine Research: An Important Component in the Fight against Tuberculosis. *BioMed Research International*, *2020*(3), 1–21. https://doi.org/10.1155/2020/4263079

Goto, A., Kadowaki, T., & Kitagawa, Y. (2003). Drosophila hemolectin gene is expressed in embryonic and larval hemocytes and its knock down causes bleeding defects. *Developmental Biology*, *264*(2), 582–591. https://doi.org/10.1016/j.ydbio.2003.06.001

Hoff, D. R., Ryan, G. J., Driver, E. R., Ssemakulu, C. C., De Groote, M. A., Basaraba, R. J., & Lenaerts, A. J. (2011). Location of Intra-and Extracellular M. tuberculosis Populations in

Lungs of Mice and Guinea Pigs during Disease Progression and after Drug Treatment. *PLoS ONE*, *6*(e17550), 1–14. https://doi.org/10.1371/journal.pone.0017550

Honti, V., Csordás, G., Kurucz, É., Márkus, R., & Andó, I. (2014). The cell-mediated immunity of Drosophila melanogaster: Hemocyte lineages, immune compartments, microanatomy and regulation. *Developmental and Comparative Immunology*, *42*(1), 47–56. https://doi.org/10.1016/j.dci.2013.06.005

Irving, P., Ubeda, J.-M., Doucet, D., Troxler, L., Lagueux, M., Zachary, D., … Meister, M. (2005). New insights into Drosophila larval haemocyte functions through genome-wide analysis. *Cellular Microbiology*, *7*(3), 335–350. https://doi.org/10.1111/j.1462-5822.2004.00462.x

Irwin, S. M., Driver, E., Lyon, E., Schrupp, C., Ryan, G., Gonzalez-Juarrero, M., … Lenaerts, A. J. (2015). Presence of multiple lesion types with vastly different microenvironments in C3HeB/FeJ mice following aerosol infection with Mycobacterium tuberculosis. *Disease Models and Mechanisms*, *8*(6), 591–602. https://doi.org/10.1242/dmm.019570

Jin, H. S., Lee, H. M., Lee, D. H., Cha, G. H., Cho, K. S., Jang, J., & Jo, E. K. (2017). Functional characterisation of the Drosophila cg6568 gene in host defence against Mycobacterium marinum. *Microbes and Infection*, *19*(6), 351–357. https://doi.org/10.1016/j.micinf.2017.02.001

Karlsson, C., Korayem, A. M., Scherfer, C., Loseva, O., Dushay, M. S., & Theopold, U. (2004). Proteomic analysis of the Drosophila larval hemolymph clot. *Journal of Biological Chemistry*, *279*(50), 52033–52041. https://doi.org/10.1074/jbc.M408220200

Kim, M. J., Wainwright, H. C., Locketz, M., Bekker, L. G., Walther, G. B., Dittrich, C., … Russell, D. G. (2010). Caseation of human tuberculosis granulomas correlates with elevated host lipid metabolism. *EMBO Molecular Medicine*, *2*(7), 258–274. https://doi.org/10.1002/emmm.201000079

Kimbrell, D. A., Hice, C., Bolduc, C., Kleinhesselink, K., & Beckingham, K. (2002). TheDorothy enhancer has tinman binding sites and driveshopscotch-induced tumor formation. *Genesis*, *34*(1–2), 23–28. https://doi.org/10.1002/gene.10134

Kjellsson, M. C., Via, L. E., Goh, A., Weiner, D., Kang, C., Low, M., … Dartois, V. (2012). Pharmacokinetic Evaluation of the Penetration of Antituberculosis Agents in Rabbit Pulmonary Lesions. *Antimicrobial Agents and Chemotherapy*, *56*(1), 446–457. https://doi.org/10.1128/AAC.05208-11

Kramnik, I., Beamer, G., & Beamer, G. (2016). Mouse models of human TB pathology : roles in the analysis of necrosis and the development of host-directed therapies. *Seminars in*

Immunopathology, *38*, 221–237. https://doi.org/10.1007/s00281-015-0538-9

Lenaerts, A. J., Hoff, D., Aly, S., Ehlers, S., Andries, K., Cantarero, L., … Basaraba, R. J. (2007). Location of Persisting Mycobacteria in a Guinea Pig Model of Tuberculosis Revealed by R207910. *Antimicrobial Agents and Chemotherapy*, *51*(9), 3338–3345. https://doi.org/10.1128/AAC.00276-07

Lesch, C., Goto, A., Lindgren, M., Bidla, G., Dushay, M. S., & Theopold, U. (2007). A role for Hemolectin in coagulation and immunity in Drosophila melanogaster. *Developmental and Comparative Immunology*, *31*(12), 1255–1263. https://doi.org/10.1016/j.dci.2007.03.012

Lindgren, M., Riazi, R., Lesch, C., Wilhelmsson, C., Theopold, U., & Dushay, M. S. (2008). Fondue and transglutaminase in the Drosophila larval clot. *Journal of Insect Physiology*, *54*(3), 586–592. https://doi.org/10.1016/j.jinsphys.2007.12.008

Makarova, O., Rodriguez-Rojas, A., Eravci, M., Weise, C., Dobson, A., Johnston, P., & Rolff, J. (2016). Antimicrobial defence and persistent infection in insects revisited. *Philosophical Transactions of the Royal Society B: Biological Sciences*, *371*(1695), 1–6. https://doi.org/10.1098/rstb.2015.0296

Marshall, J. (2011). Cell Migration Transwell Assay. *Methods*, *769*(4), 111–136. https://doi.org/10.1007/978-1-61779-207-6

Marzo, E., Vilaplana, C., Tapia, G., Diaz, J., Garcia, V., & Cardona, P.-J. (2014). Damaging role of neutrophilic infiltration in a mouse model of progressive tuberculosis. *Tuberculosis*, *94*(1), 55–64. https://doi.org/10.1016/j.tube.2013.09.004

Meister, M., Lemaitre, B., & Hoffmann, J. A. (1997). Antimicrobial peptide defense in Drosophila. *BioEssays*, *19*(11), 1019–1026. https://doi.org/10.1002/bies.950191112

Mitchell, G., Chen, C., & Portnoy, D. A. (2016). Strategies Used by Bacteria to Grow in Macrophages. *Microbiology Spectrum*, *4*(3), 1–22. https://doi.org/10.1128/microbiolspec.MCHD-0012-2015

Mulcahy, H., Sibley, C. D., Surette, M. G., & Lewenza, S. (2011). Drosophila melanogaster as an animal model for the study of Pseudomonas aeruginosa biofilm infections in Vivo. *PLoS Pathogens*, *7*(10), 1–14. https://doi.org/10.1371/journal.ppat.1002299

Nam, H., Jang, I., You, H., Lee, K., & Lee, W. (2012). Genetic evidence of a redox-dependent systemic wound response via Hayan Protease- Phenoloxidase system in Drosophila. *The EMBO Journal*, *31*(5), 1253–1265. https://doi.org/10.1038/emboj.2011.476

Nascimento, M. T. C., Silva, K. P., Garcia, M. C. F., Medeiros, M. N., Machado, E. A., Nascimento, S. B., & Saraiva, E. M. (2018). DNA extracellular traps are part of the immune repertoire of Periplaneta americana. *Developmental and Comparative*

Immunology, *84*, 62–70. https://doi.org/10.1016/j.dci.2018.01.012

Oh, C. T., Moon, C., Choi, T. H., Kim, B. S., & Jang, J. (2013). Mycobacterium marinum infection in Drosophila melanogaster for antimycobacterial activity assessment. *Journal of Antimicrobial Chemotherapy*, *68*(3), 601–609. https://doi.org/10.1093/jac/dks425

Osherov, N., & Ben-Ami, R. (2016). Modulation of Host Angiogenesis as a Microbial Survival Strategy and Therapeutic Target. *PLoS Pathogens*, *12*(4), 1–8. https://doi.org/10.1371/journal.ppat.1005479

Peán, C. B., Schiebler, M., Tan, S. W. S., Sharrock, J. A., Kierdorf, K., Brown, K. P., … Dionne, M. S. (2017). Regulation of phagocyte triglyceride by a STAT-ATG2 pathway controls mycobacterial infection. *Nature Communications*, *8*(14642), 1–11. https://doi.org/10.1038/ncomms14642

Pham, L. N., Dionne, M. S., Shirasu-Hiza, M., & Schneider, D. S. (2007). A specific primed immune response in Drosophila is dependent on phagocytes. *PLoS Pathogens*, *3*(3), e26. https://doi.org/10.1371/journal.ppat.0030026

Prats, C., Vilaplana, C., Valls, J., Marzo, E., & Cardona, P. (2016). Local Inflammation , Dissemination and Coalescence of Lesions Are Key for the Progression toward Active Tuberculosis : The Bubble Model. *Frontiers in Microbiology*, *7*(33), 1–11. https://doi.org/10.3389/fmicb.2016.00033

Qian, X., Nguyen, D. T., Lyu, J., Albers, A. E., Bi, X., & Graviss, E. A. (2018). Risk factors for extrapulmonary dissemination of tuberculosis and associated mortality during treatment for extrapulmonary tuberculosis. *Emerging Microbes & Infections*, *7*(102). https://doi.org/10.1038/s41426-018-0106-1

Raviglione, M., & Sulis, G. (2016). Tuberculosis 2015: burden, challenges and strategy for control and elimination. *Infectious Disease Reports*, *8*(6570), 33–37. https://doi.org/10.4081/idr.2016.6570

Russell, D. G. (2007). Who puts the tubercle in tuberculosis? *Nature Reviews Microbiology*, *5*(1), 39–47. https://doi.org/10.1038/nrmicro1538

Russell, D. G., Cardona, P.-J., Kim, M.-J., Allain, S., & Altare, F. (2009). Foamy macrophages and the progression of the human TB granuloma. *Nature Immunology*, *10*(9), 943–948. https://doi.org/10.1038/ni.1781

Ryu, J., Kim, S., Lee, H., Bai, J. Y., Nam, Y., Bae, J., … Lee, W. (2008). Innate Immune Homeostasis by the Homeobox Gene Caudal and Commensal-Gut Mutualism in Drosophila. *Science*, *319*(5864), 777–782. https://doi.org/10.1126/science.1149357

Scherfer, C., Karlsson, C., Loseva, O., Bidla, G., Goto, A., Havemann, J., … Theopold, U.

(2004). Isolation and Characterization of Hemolymph Clotting Factors in Drosophila melanogaster by Pullout Method. *Current Biology*, *14*, 625–629. https://doi.org/10.1016/j.cub.2004.03.030 Isolation

Scherfer, C., Qazi, M. R., Takahashi, K., Ueda, R., Dushay, M. S., Theopold, U., & Lemaitre, B. (2006). The Toll immune-regulated Drosophila protein Fondue is involved in hemolymph clotting and puparium formation, *295*, 156–163. https://doi.org/10.1016/j.ydbio.2006.03.019

Schnappinger, D., & Ehrt, S. (2016). A broader spectrum of tuberculosis. *Nature Medicine*, *22*(10), 1076–1077. https://doi.org/10.1038/nm.4186

Scriba, T. J., Coussens, A. K., & Fletcher, H. A. (2017). Human Immunology of Tuberculosis. *Microbiology Spectrum*, *5*(1), 1–24. https://doi.org/10.1128/microbiolspec.TBTB2-0016-2016

Shia, A. K. H., Glittenberg, M., Thompson, G., Weber, A. N., Reichhart, J. M., & Ligoxygakis, P. (2009). Toll-dependent antimicrobial responses in Drosophila larval fat body require Spätzle secreted by haemocytes. *Journal of Cell Science*, *122*(24), 4505–4515. https://doi.org/10.1242/jcs.049155

Singh, A. K., & Gupta, U. D. (2018). Animal models of tuberculosis: Lesson learnt. *Indian Journal of Medical Research*, *147*(5), 456–463. https://doi.org/10.4103/ijmr.IJMR_554_18

Sorvina, A., Brooks, D. A., Ng, Y. S., Bader, C. A., Weigert, R., & Shandala, T. (2013). Bacterial challenge initiates endosome-lysosome response in Dr o sophila immune tissues. *IntraVital*, *2*(1), 1–12. https://doi.org/10.4161/intv.23889

Sugumaran, M. (2002). Comparative Biochemistry of Eumelanogenesis and the Protective Roles of Phenoloxidase and Melanin in Insects. *Pigment Cell Research*, *15*(1), 2–9. https://doi.org/10.1034/j.1600-0749.2002.00056.x

Suki, B., Sato, S., Szabari, M. V., Takahashi, A., Parameswaran, H., & Bartolák-suki, E. (2013). Emphysema and Mechanical Stress-Induced Lung Remodeling. *Physiology*, *28*(36), 404–413. https://doi.org/10.1152/physiol.00041.2013

Theopold, U., Krautz, R., & Dushay, M. S. (2014). The Drosophila clotting system and its messages for mammals. *Developmental and Comparative Immunology*, *42*(1), 42–46. https://doi.org/10.1016/j.dci.2013.03.014

Tzou, P., Ohresser, S., Ferrandon, D., Capovilla, M., Reichhart, J., Lemaitre, B., … Mole, I. D. B. (2000). Tissue-Specific Inducible Expression of Antimicrobial Peptide Genes in Drosophila Surface Epithelia. *Immunity*, *13*(5), 737–748.

https://doi.org/doi:10.1016/s1074-7613(00)00072-8

Ulrichs, T., & Kaufmann, S. H. (2006). New insights into the function of granulomas in human tuberculosis. *The Journal of Pathology*, *208*(2), 261–269. https://doi.org/10.1002/path.1906

Vlisidou, I., & Wood, W. (2015). Drosophila blood cells and their role in immune responses. *FEBS Journal*, *282*(8), 1368–1382. https://doi.org/10.1111/febs.13235

Wang, X., Aliyari, R., Li, W., Li, H., Kim, K., Carthew, R., … Ding, S. (2006). RNA Interference Directs Innate Adult Drosophila. *Science*, *312*(5772), 452–455. https://doi.org/10.1126/science.1125694

Wang, Z., Wilhelmsson, C., Hyrsl, P., Loof, T. G., Dobes, P., Klupp, M., … Theopold, U. (2010). Pathogen entrapment by transglutaminase - A conserved early innate immune mechanism. *PLoS Pathogens*, *6*(2), e1000763. https://doi.org/10.1371/journal.ppat.1000763

Williams, A., & Orme, I. M. (2016). Animal Models of Tuberculosis: An Overview. *Microbiology Spectrum*, *4*(4), 1–12. https://doi.org/10.1128/microbiolspec.TBTB2-0004-2015

Wolf, A. J., Desvignes, L., Linas, B., Banaiee, N., Tamura, T., Takatsu, K., & Ernst, J. D. (2008). Initiation of the adaptive immune response to Mycobacterium tuberculosis depends on antigen production in the local lymph node, not the lungs. *Journal of Experimental Medicine*, *205*(1), 105–115. https://doi.org/10.1084/jem.20071367

Zabihihesari, A., Hilliker, A. J., & Rezai, P. (2020). Localized microinjection of intact: Drosophila melanogaster larva to investigate the effect of serotonin on heart rate. *Lab on a Chip*, *20*(2), 343–355. https://doi.org/10.1039/c9lc00963a

Zsámboki, J., Csordás, G., Honti, V., Pintér, L., Bajusz, I., Galgóczy, L., … Kurucz, É. (2013). Drosophila Nimrod proteins bind bacteria. *Central European Journal of Biology*, *8*(7), 633–645. https://doi.org/10.2478/s11535-013-0183-4

9. Annexes

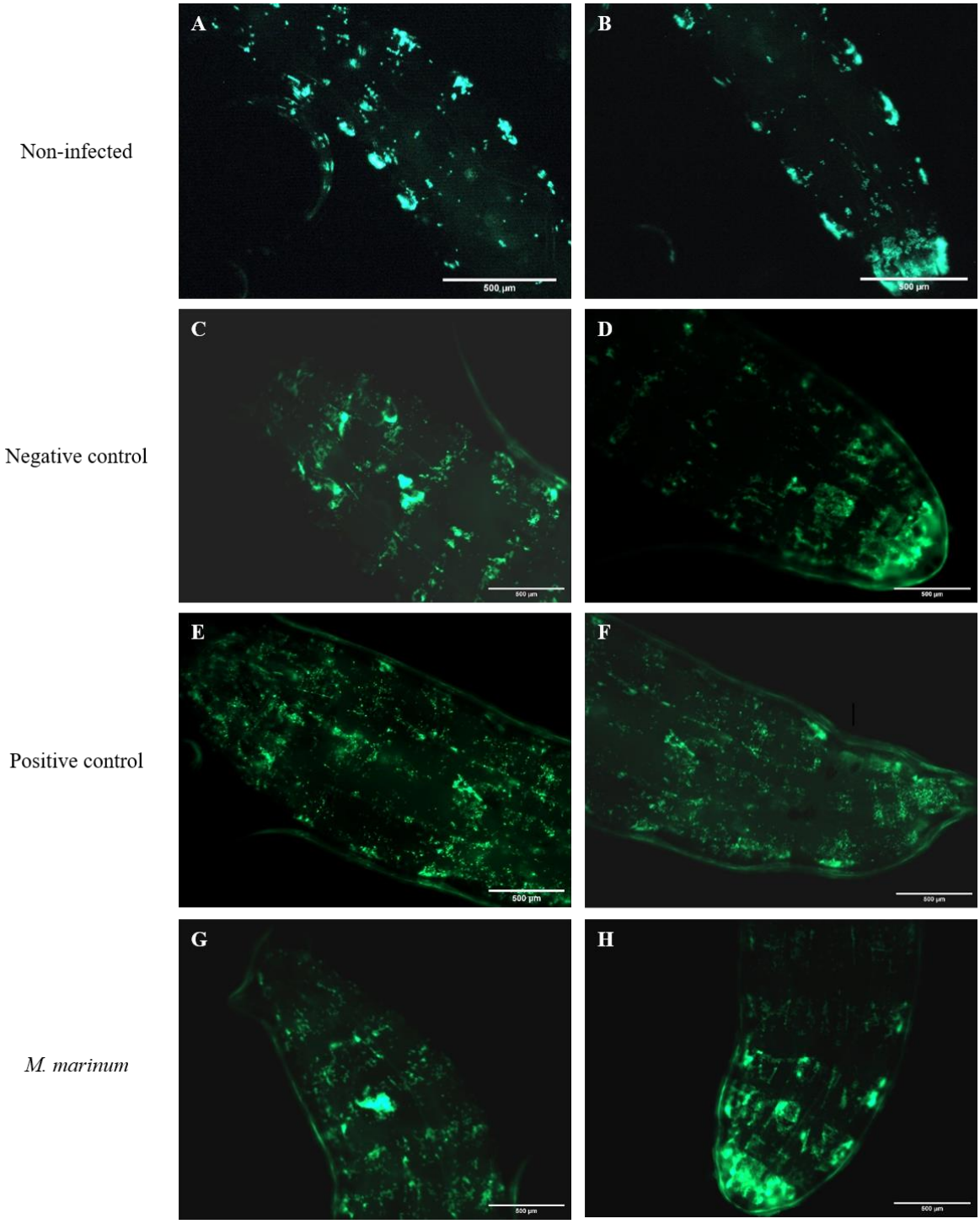

Figure A1: Imaging of live third instar *Drosophila* larvae at 24hpi performed with fluorescent microscopy at 10x. Larvae were placed with the dorsal side facing up. White arrows indicate the localization of the Figures (Fig A2) presented below and green represents GFP-hemolectin hemocytes. (A and B) Hemocyte distribution of a non-injected third instar *Drosophila* larvae. Hemocytes are mainly localized in the sessile hematopoietic tissue and their respective lateral pockets (C and D) Hemocyte distribution observed at the anterior and posterior part of *Drosophila* larva infected with LPS, respectively. (E and F) Hemocyte distribution visualized respectively at the anterior and posterior halves of *Drosophila* larva infected with *M. marinum.* (G and H) Imaging of the hemocyte distribution of both anterior and posterior portions of the negative control *Drosophila* larva.

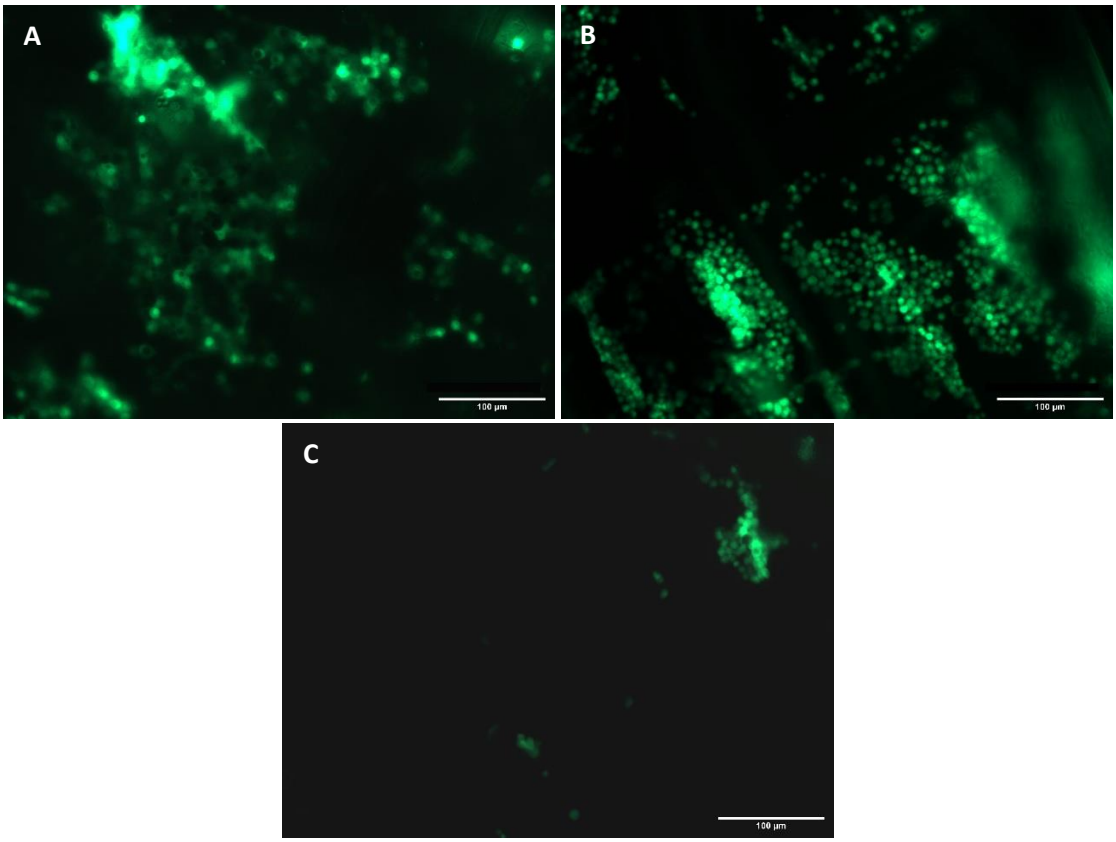

Figure A2: Imaging of live third instar *Drosophila* larvae at 24hpi performed with fluorescent microscopy at 20x. Localization of the hemocytes seen in the images is indicated by the white arrows present in Fig. A1 for each infection group. Hemocytes morphology and distribution of *Drosophila* larva infected with LPS (A), *M. marinum* (B), and PBS (C). Higher induction of circulating hemocytes is seen in images A and B. Moreover, hemocytes seen in image B show less morphological changes after infection in comparison hemocytes seen in image A.

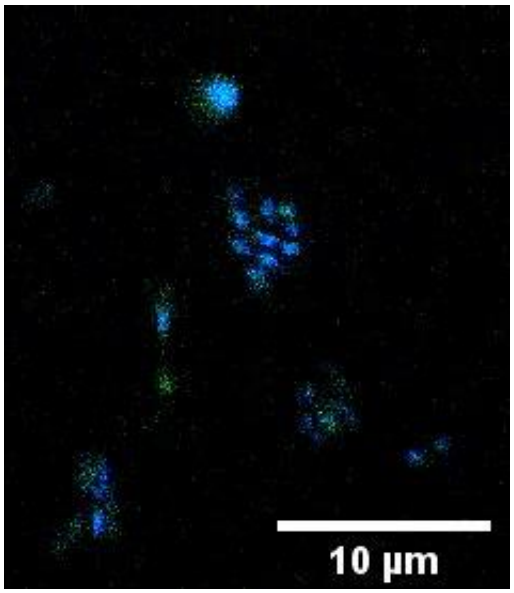

Fig A3. Clotting formation analysis of extracted hemolymph at 24 hours post *in vivo* infection of third instar *Drosophila* larvae. Imaging was performed by confocal microscopy at 100x. Green represents hemocytes expressing GFP-hemolectin and blue is DAPI stained DNA.

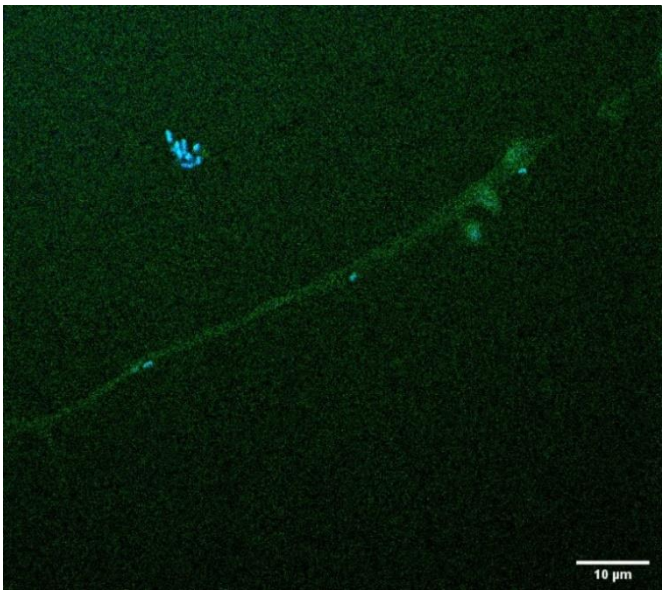

Fig A4. Imaging of unknown source of contamination. Imaging obtained from hemolymph extracted at 24 hours post *in vivo* infection and obtained through confocal microscopy at 100x. Green represents hemocytes expressing GFP-hemolectin, and blue is DNA stained with DAPI. Ellipsoidal (white arrow) and filament (orange arrow) shaped structures are barely intuited in green fluorescence.

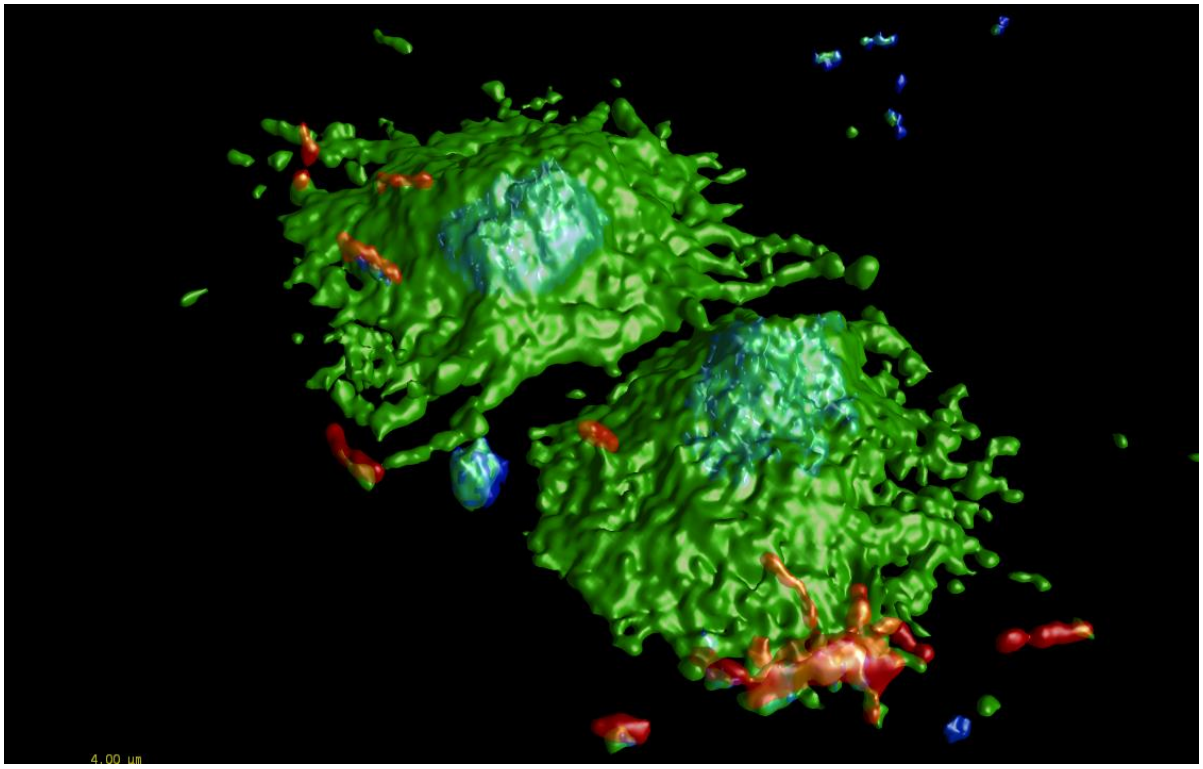

Fig A5. Tridimensional representation of Fig. 2C.